Vet Pathol **45**:551–562 (2008)

Pathology of Experimental SARS Coronavirus Infection in Cats and Ferrets

J. M. A. van den Brand, B. L. Haagmans, L. Leijten, D. van Riel, B. E. E. Martina, A. D. M. E. Osterhaus, and T. Kuiken

Department of Virology, Erasmus Medical Center, Rotterdam, the Netherlands

Abstract. The pathology of severe acute respiratory syndrome-coronavirus (SARS-CoV) infection in cats and ferrets is poorly described, and the distribution of angiotensin-converting enzyme 2 (ACE2), a receptor for SARS-CoV, in the respiratory tracts of these species is unknown. We observed SARS-CoV antigen expression and lesions in the respiratory tracts of 4 cats and 4 ferrets at 4 days postinoculation and ACE2 expression in the respiratory tracts of 3 cats and 3 ferrets without infection. All infected cats and ferrets had diffuse alveolar damage associated with SARS-CoV antigen expression. A novel SARS-CoV–associated lesion was tracheo-bronchoadenitis in cats. SARS-CoV antigen expression occurred mainly in type I and II pneumocytes and serous cells of tracheo-bronchial submucosal glands of cats and in type II pneumocytes of ferrets. ACE2 expression occurred mainly in type I and II pneumocytes, tracheo-bronchial goblet cells, serous epithelial cells of tracheo-bronchial submucosal glands in cats, and type II pneumocytes and serous epithelial cells of tracheo-bronchial submucosal glands in ferrets. In conclusion, the pathology of SARS-CoV infection in cats and ferrets resembles that in humans except that syncytia and hyaline membranes were not observed. The identification of tracheo-bronchoadenitis in cats has potential implications for SARS pathogenesis and SARS-CoV excretion. Finally, these results show the importance of ACE2 expression for SARS-CoV infection in vivo: whereas ACE2 expression in type I and II pneumocytes in cats corresponded to SARS-CoV antigen expression in both cell types, expression of both ACE2 and SARS-CoV antigen in ferrets was limited mainly to type II pneumocytes.

Key words: Angiotensin-converting enzyme (ACE2); cats; coronavirus; ferrets; histology; immunohistochemistry; respiratory system; severe acute respiratory syndrome (SARS).

Severe acute respiratory syndrome (SARS) emerged in the human population in November 2002 and spread rapidly across Asia, Europe, and North America in subsequent months.[29] Although the causative virus, SARS-coronavirus (SARS-CoV),[5,6,19,28] was eradicated from the human population by July 2003, its progenitors are likely still present in animal reservoirs[21] and could again cross the species barrier into humans. In total, SARS caused 774 deaths out of more than 8,000 people with confirmed infection. Because the pathogenesis of SARS in humans is poorly understood, it is difficult to develop preventive and therapeutic strategies against this disease.[29]

The primary lesion of SARS in humans is diffuse alveolar damage (DAD), indicating injury to the alveolar septa.[4,7,12,25,27] This lesion corresponds in part to the cell types in the respiratory tract in which SARS-CoV antigen has been detected: alveolar epithelial cells (primarily type II pneumocytes), bronchial epithelial cells, and alveolar macrophages.[3,29,33,38,40] Cases of longer duration (more than 10 days) demonstrated features of organizing-phase or late-stage DAD.[7,27]

Angiotensin-converting enzyme 2 (ACE2) has been identified as a receptor for the attachment to and uptake of SARS-CoV in host cells.[20] The distribution of ACE2 in human tissues corresponds largely to the cell types in which SARS-CoV replication has been observed: in addition to type II pneumocytes and bronchial epithelial cells, ACE2 expression has been observed in type I pneumocytes and endothelial cells as well as smooth muscle cells of blood vessels, but not alveolar macrophages.[15,37]

Since the appearance of SARS, several animal models have been developed for SARS-CoV infection in humans: SARS-CoV infection in

macaques,[6] marmosets,[10] mice,[8,31] golden Syrian hamsters,[32] rats,[24] cats, and ferrets.[22] Subbarao and Roberts[35] reviewed the advantages and disadvantages of the above animal models. The limitations of rodents such as hamsters and young inbred mice are that they do not show illness[35] and their lung structure differs from that of the human lung;[26] the limitations of nonhuman primates are availability, cost, and housing.[35] SARS-CoV infections in cats and ferrets do not show these limitations and may therefore be valuable as animal models.

Previous experiments showed that domestic cats and ferrets were susceptible to SARS-CoV infection and that they were able to transmit the virus efficiently to previously uninfected sentinel animals that were housed with them.[22] The acute pulmonary lesions seen in those species were reported to be similar to those in humans and macaques, but were not described.[22,36] Chronic lesions in ferrets euthanized at 23 days after infection were bronchial and bronchiolar hyperplasia as well as peribronchiolar and perivascular lymphocytic cuffing.[1,2] However, the pathology and viral distribution in cats and ferrets with acute SARS-CoV infection are poorly understood.

Our goal was to describe the pathology of acute SARS-CoV infection in cats and ferrets and to determine the expression of ACE2 in the respiratory tracts of these species. Therefore, we experimentally infected cats and ferrets with SARS-CoV and examined respiratory tract tissues at 4 days postinoculation (d.p.i.) by histopathology, immunohistochemistry, and immunofluorescence.

Materials and Methods

Virus preparation

Strain HKU 39849 of SARS-CoV was passaged 4 times on Vero 118 cells cultured in Iscove's Modified Dulbeco's Medium (Bio Whitaker, Walkersville, MD). After centrifugation at 270 × *g* for 5 minutes, 1 ml samples were made from the supernatant and the pelleted cells, and were resuspended in 5 ml medium. The titer of this virus stock was 1×10^6 median tissue culture infectious dose ($TCID_{50}$) per ml. All cell cultures were done under biosafety level 3 conditions.

Experimental protocol

The experiments were performed under biosafety level 3 conditions at the Erasmus Medical Center in Rotterdam under an animal study protocol approved by the Institutional Animal Welfare Committee. Specified-pathogen-free cats and ferrets were purchased from commercial breeders (Harlan, Indianapolis, IN and Schimmel, Uddel, The Netherlands, respectively), maintained in standard housing, and provided with commercial food pellets and water ad libitum until the start of the experiment. Before infection, they were examined clinically and determined to be healthy by a registered veterinarian and were placed in negative-pressurized glove boxes. Four cats and 4 ferrets were inoculated intratracheally in 1–5 seconds under ketamine anesthesia with 10^6 $TCID_{50}$ of SARS-CoV. The animals were checked daily for clinical signs. At 4 days d.p.i., they were euthanized by exsanguination under ketamine anesthesia. Three cats and 3 ferrets were not inoculated and were used as negative controls.

Pathologic examination

The animals were necropsied according to a standard protocol by opening the thoracic and abdominal cavities and the skull and examining all major organs, including the brain. Samples were collected for histologic examination and were stored in 10% neutral-buffered formalin (lungs after inflation with formalin), embedded in paraffin, sectioned at 4 μm, and stained with HE for examination by light microscopy. Selected lung sections also were stained with periodic acid Schiff (PAS) for detection of mucoid substances. The following tissues were examined by light microscopy: lung (cranial, middle, and caudal lobes of one lung), liver, spleen, kidney, trachea, urinary bladder, mesenteric lymph node, stomach (ferrets only), pancreas, duodenum, jejunum, ileum, and tracheo-bronchial lymph node. Semiquantitative assessment of SARS-CoV infection–associated inflammation in the lung was performed as reported earlier:[14] each slide was examined for inflammatory foci at 10× objective, and each focus was scored for size (1] smaller or equal than area of 10× objective, 2] larger than area of 10× objective and smaller than area of 2× objective, and 3] larger than area of 2× objective) and severity of inflammation (1] mild, 2] moderate, and 3] marked). Slides were examined without knowledge of the identity of the animals. The cumulative scores for the inflammatory foci provided the total score per animal.

Immunohistochemistry

Immunohistochemical examination on all tissues as examined by using light microscopy was performed as reported previously,[19] except that mouse anti-SARS-nucleocapsid IgG2a (clone Ncap4, Imgenex, San Diego, CA, USA) (0.3 μg/ml) and goat anti-mouse IgG2a (SouthernBiotech, Birmingham, AL, USA) were used as primary and secondary antibodies, respectively. Omission of the primary antibody or replacement of the primary antibody by an irrelevant mouse IgG2a antibody (clone 20102, R&D, Abingdon, UK) (0.3 μg/ml) were included as negative controls in each staining. The same tissues as mentioned above from noninfected cats and ferrets were used as negative controls. Lung sections from an experimentally inoculated ferret euthanized on 1 d.p.i. were used as positive controls. Semiquantitative assessment of SARS-CoV antigen expression was performed as reported earlier:[14] 25 arbitrarily chosen 20× objective fields of lung parenchyma in each lung section were examined by using light

microscopy for the presence of SARS-CoV antigen expression, without the knowledge of the identity of the animals. The cumulative scores for each animal were expressed as the number of positive fields per 100 fields.

For double staining of SARS-CoV antigen and PAS-positive material, staining for SARS-CoV antigen was performed as described above with the following modifications. Antigen retrieval was performed at 100°C for 15 minutes with citric acid buffer, pH 6.0. Sections were cooled for 20 minutes on ice in the same buffer. To allow double staining, mouse anti-SARS-nucleocapsid IgG1 (Ncap17, Imgenex) (1.25 μg/ml) and biotin-labeled goat anti-mouse IgG1 (SouthernBiotech) were used as primary and secondary antibodies, respectively. After incubation with the secondary antibody, the labeled biotin was coupled to avidin-biotin-HRP complexes (DAKO, Heverlee, Belgium) for 1 hour at room temperature. Peroxidase activity was revealed by incubating slides in 3,3′–diaminobenzidine-tetrachlorhydrate (Sigma, St Louis, MO) for 3 to 5 minutes, resulting in a brown precipitate. After washing in phosphate buffered saline (PBS), slides were stained with PAS according to standard methods.

For detection of ACE2, tissue sections were pretreated as described above and incubated with a rabbit polyclonal antibody to ACE2 (Abcam, Cambridge, UK) (5 μg/ml) or rabbit IgG control (R&D) (5 μg/ml) in PBS/0.1% body surface area (BSA) for 1 hour at room temperature. After washing with PBS, sections were incubated with HRP-labeled goat-anti-rabbit IgG (DAKO) in PBS/0.1% BSA for 1 hour at room temperature. Peroxidase activity was revealed by incubating slides in 3-amino-9-ethylcarbazole (Sigma) for 10 minutes and counterstaining with hematoxylin.

To identify the ACE2 expression at the time of infection, we used the 3 noninfected cats and 3 noninfected ferrets, since spike protein binding during SARS-CoV infection results in down-regulation of ACE2 expression.[18] For comparison of ACE2 expression and histologic architecture of the tracheal submucosal glands among cats, ferrets, and humans, archival human tracheal tissues of 3 individuals, without histologic lesions or evidence of respiratory tract infection at the time of death, also were stained with PAS and tested for ACE2 expression.

Immunofluorescence

For double staining of SARS-CoV antigen and keratin, 3-μm-thick, formalin-fixed, paraffin-embedded tissue sections were pretreated as described above. Autofluorescence in the sections was blocked by incubation with 0.3 M glycine for 10 minutes. Sections were washed with PBS/0.05% Tween 20 and incubated with mouse IgG1 against human pankeratin AE1/AE3 (Neomarkers, Fremont, CA) (8 μg/ml) for 1 hour at room temperature in the dark. After washing with PBS, sections were incubated with mouse IgG1 against SARS-CoV (clone Ncap17, Imgenex) (1.25 μg/ml) for 1 hour at room temperature in the dark. The pankeratin antibody was labeled by using the Zenon Alexa Fluor 488 Mouse IgG1 labeling kit (cat. no. Z25090, Molecular Probes, Invitrogen, Breda, The Netherlands) according to the manufacturer's protocol. The SARS-CoV antibody was labeled by using a Zenon Alexa Fluor 594 Mouse IgG1 labeling kit (cat. no. Z25007, Molecular Probes). The slides were mounted by using the Vectashield, hard set with 4,6-diamidino-2-phenylindole (Vector, Burlingame, CA).

Statistical analysis

One-way analysis of variance was used for comparing the scores of pulmonary lesions and viral antigen expression. Differences were considered significant at $P < .05$.

Results

Clinical findings

The cats showed no clinical signs such as lethargy or dyspnea. The ferrets, however, became lethargic from 2 d.p.i. onward, and 1 of these ferrets (No. 3) died at 4 d.p.i.

Gross examination

All 4 cats had multifocal pulmonary consolidation characterized by red, firm, level areas of approximately 1 cm in diameter in the cranial and medial lobes. Cat No. 4 had multifocal consolidation in all lung lobes. All 4 ferrets also had multifocal pulmonary consolidation similar to that in the cats, except that the foci were smaller, ranging from 0.1 to 1 cm in diameter, and were localized mainly in the caudal lobes. Ferret No. 2 also had dark red and enlarged mesenteric lymph nodes, and ferret No. 3 had a dark red, friable liver and a mottled, red-and-pink spleen. Other organs of the cats and ferrets showed no significant lesions.

Histology

The primary damage from SARS-CoV infection was seen in the respiratory tract in both cats and ferrets and was comparable in character and severity. In the cats, histologic lesions were seen in the lung, tracheo-bronchial submucosal glands, spleen, tracheo-bronchial and mesenteric lymph nodes, and Peyer's patches (Figs. 1–4). In the lung, all cats had multifocal, mild-to-moderate, exudative DAD characterized by cellular debris in the alveolar lumen and epithelial cells with karyorrhexis, karyopyknosis, and loss of cellular detail (multifocal necrosis), sparse type II pneumocyte hyperplasia, and infiltration with few neutrophils in the alveolar septa (Fig. 4). In the lumina of terminal bronchioles and adjacent alveoli, there were few alveolar macrophages and neutrophils (Figs. 3, 4). In the tracheo-bronchial submucosal

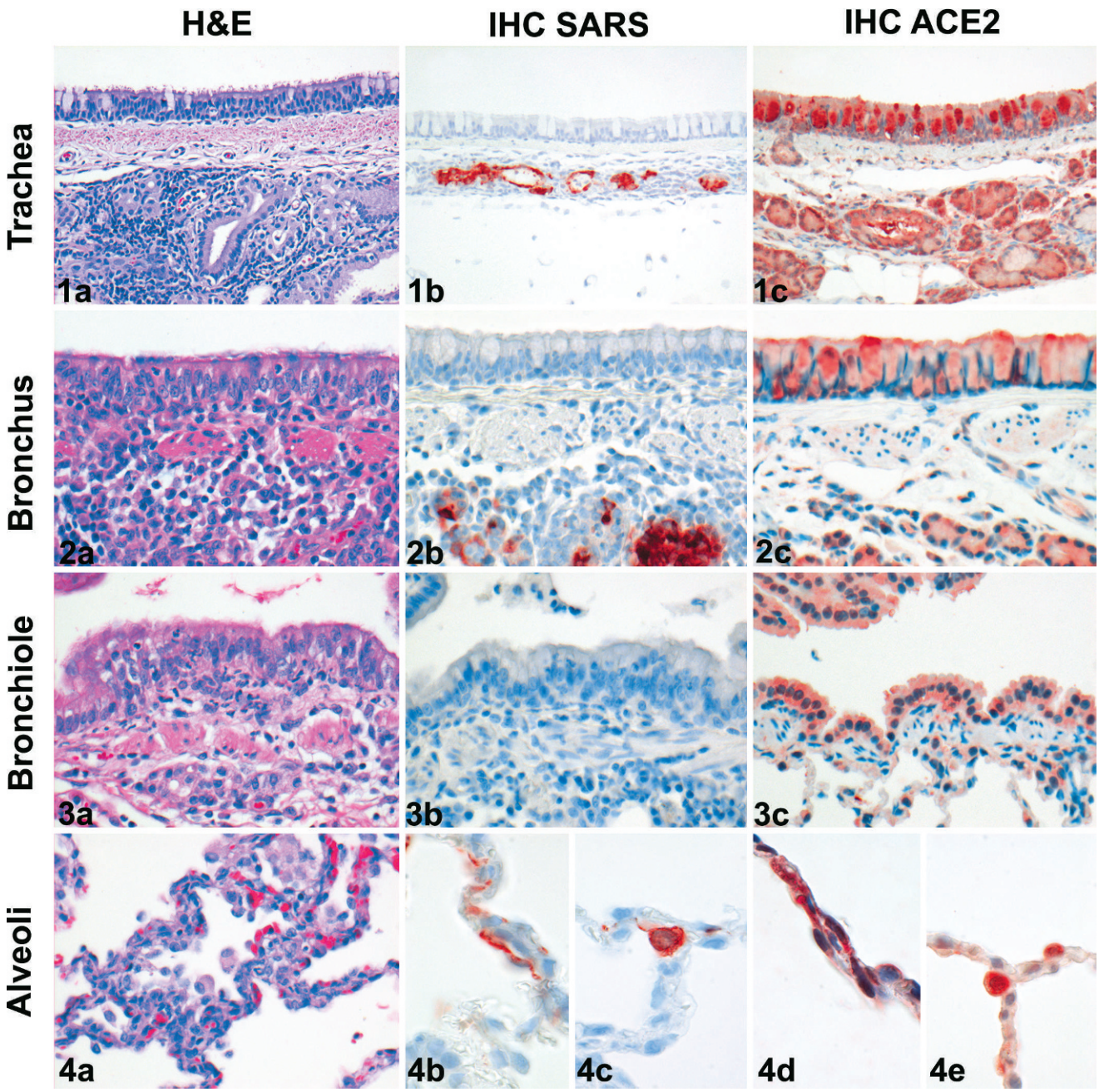

Figs. 1–4. Respiratory tract. Histologic and immunohistochemical staining for SARS-CoV antigen and ACE2 in SARS-CoV–infected cats and control cats. Detailed descriptions can be found in the text. **Fig. 1a.** Trachea; cat No. 2. Moderate lymphoplasmacytic tracheoadenitis. HE. **Fig. 1b.** Trachea; cat No. 2. SARS-CoV antigen expression in epithelial cells of submucosal glands. Immunoperoxidase with hematoxylin counterstain. **Fig. 1c.** Trachea; control cat. ACE2 expression in epithelial cells of mucosa and submucosal glands. Immunoperoxidase with hematoxylin counterstain. **Fig. 2a.** Bronchus; cat No. 1. Moderate lymphoplasmacytic bronchoadenitis. HE. **Fig. 2b.** Bronchus; cat No. 1. SARS-CoV antigen expression in epithelial cells of submucosal glands. Immunoperoxidase with hematoxylin counterstain. **Fig. 2c.** Bronchus; control cat. ACE2 expression in epithelial cells of mucosa and submucosal glands. Immunoperoxidase with hematoxylin counterstain. **Fig. 3a.** Bronchiole; cat No. 1. Mild lymphoplasmacytic and neutrophilic bronchiolitis. HE. **Fig. 3b.** Bronchiole; cat No. 1. Lack of SARS-CoV antigen expression. Immunoperoxidase with hematoxylin counterstain. **Fig. 3c.** Bronchiole; control cat. ACE2 expression in epithelial cells of mucosa. Immunoperoxidase with hematoxylin counterstain. **Fig. 4a.** Alveoli; cat No. 4. Mild DAD. HE. **Figs. 4b, c.** Alveoli; cat No. 3. SARS-CoV antigen expression in type I (k) and II (l) pneumocytes. Immunoperoxidase with hematoxylin counterstain. **Figs. 4d, e.** Alveoli; control cat. ACE2 expression in type I (m) and II (n) pneumocytes. Immunoperoxidase with hematoxylin counterstain.

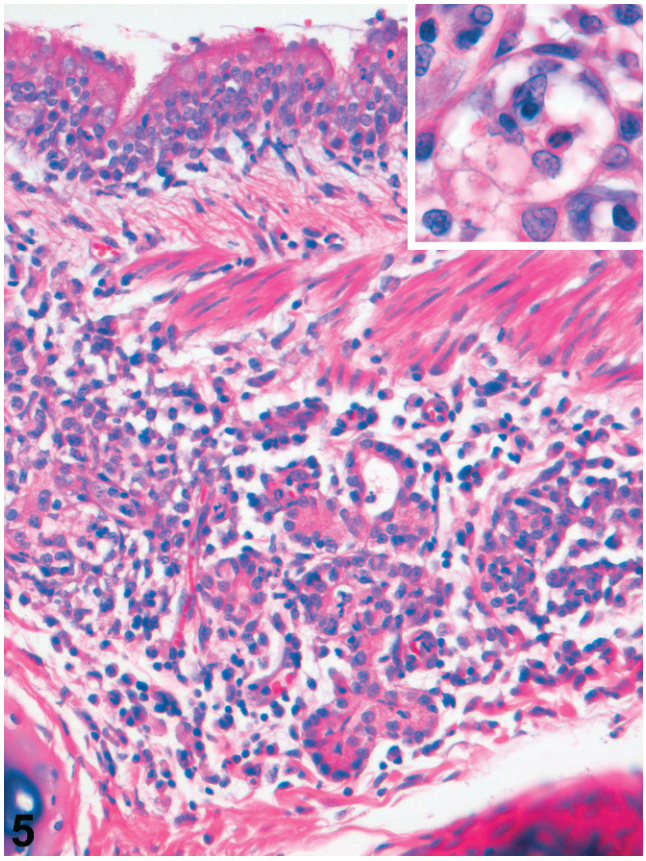

Fig. 5. Bronchus; cat No. 1. Histologic staining of a bronchus in a cat infected with SARS-CoV. Moderate lymphoplasmacytic bronchoadenitis with mild necrosis of glandular epithelial cells. HE. *Inset:* Higher magnification of a submucosal gland with loss of epithelial cells.

glands, all cats had multifocal, mild-to-moderate tracheo-bronchoadenitis (Figs. 1, 2, 5, 6). This was characterized by multifocal epithelial necrosis in submucosal glands and by infiltration with moderate numbers of plasma cells and lymphocytes and with few macrophages and neutrophils in surrounding connective tissue. With PAS staining, these submucosal glands displayed narrow, empty lumina, a high proportion of serous cells compared with mucous cells, and mild granular PAS staining in mucous cells (Figs. 6, 7), which was also seen in noninfected cats. In cats Nos. 1 and 3, the spleen had moderate lymphoid hyperplasia, while tracheo-bronchial and mesenteric lymph nodes and Peyer's patches had both mild-to-moderate lymphoid hyperplasia and moderate-to-marked sinusoidal histiocytosis. No significant lesions were seen in other tissues examined or in the tissues of the negative control cats.

In the ferrets, histologic lesions were seen in the lung, liver, spleen, and tracheo-bronchial lymph nodes (Figs. 8–11). In the lung, all ferrets had multifocal, mild-to-severe, subacute, exudative DAD characterized by variable numbers of alveolar macrophages and neutrophils, mixed with proteinaceous exudate in alveolar and bronchiolar lumina (Fig. 11). The alveolar septa were moderately thickened with infiltrating neutrophils, macrophages, and multifocal moderate epithelial necrosis (Fig. 11). There was multifocal hyperplasia and hypertrophy of type II pneumocytes and bronchiolar epithelial cells (Fig. 10). There was hyperplasia of bronchus-associated lymphoid tissue, and additionally, ferret No. 3 had lymphoid aggregates around pulmonary blood vessels. Overall, the severity of pulmonary lesions in the ferrets and cats showed no significant differences ($F = 0.48$, $P = .51$) (Fig. 12). In the liver, all ferrets had mild diffuse hepatic lipidosis, while ferret No. 3 also had mild diffuse hepatic congestion and hemorrhage. The spleen and tracheo-bronchial lymph nodes of all ferrets showed mild lymphoid hyperplasia. In contrast to the cats, no significant lesions were seen in the tracheo-bronchial submucosal glands of the ferrets (Fig. 8). PAS staining of these glands (in both infected and noninfected animals) showed wide lumina filled with PAS-positive material, a low proportion of serous cells compared with mucous cells, and intense, diffuse PAS-expression in mucous cells (Figs. 6, 7). No significant lesions were seen in other tissues examined or in the tissues of negative control ferrets.

In human tissues, the tracheal and bronchial submucosal glands had an almost equal mixture of serous and mucous cells. The lumina varied in size, and some were filled with large amounts of PAS-positive material.

SARS-CoV antigen expression

The cell types expressing SARS-CoV antigen, visible as diffuse red staining of the cytoplasm, differed between cats and ferrets (Table 1, Figs. 1–4, 8–11). In cats, SARS-CoV antigen expression was limited to the respiratory tract and the intestine. In the respiratory tract of all cats, SARS-CoV antigen expression was seen mainly in type I pneumocytes, type II pneumocytes (Fig. 4), and serous cells of the tracheo-bronchial submucosal glands (Figs. 1, 2); occasionally in alveolar macrophages; and rarely in tracheal, bronchial, and (Cat No. 3 only) bronchiolar ciliated epithelial cells. The identity of SARS-CoV-antigen-positive type I and type II pneumocytes was based on their morphology (flat and cuboidal, respectively) and confirmed by double staining with pankeratin to

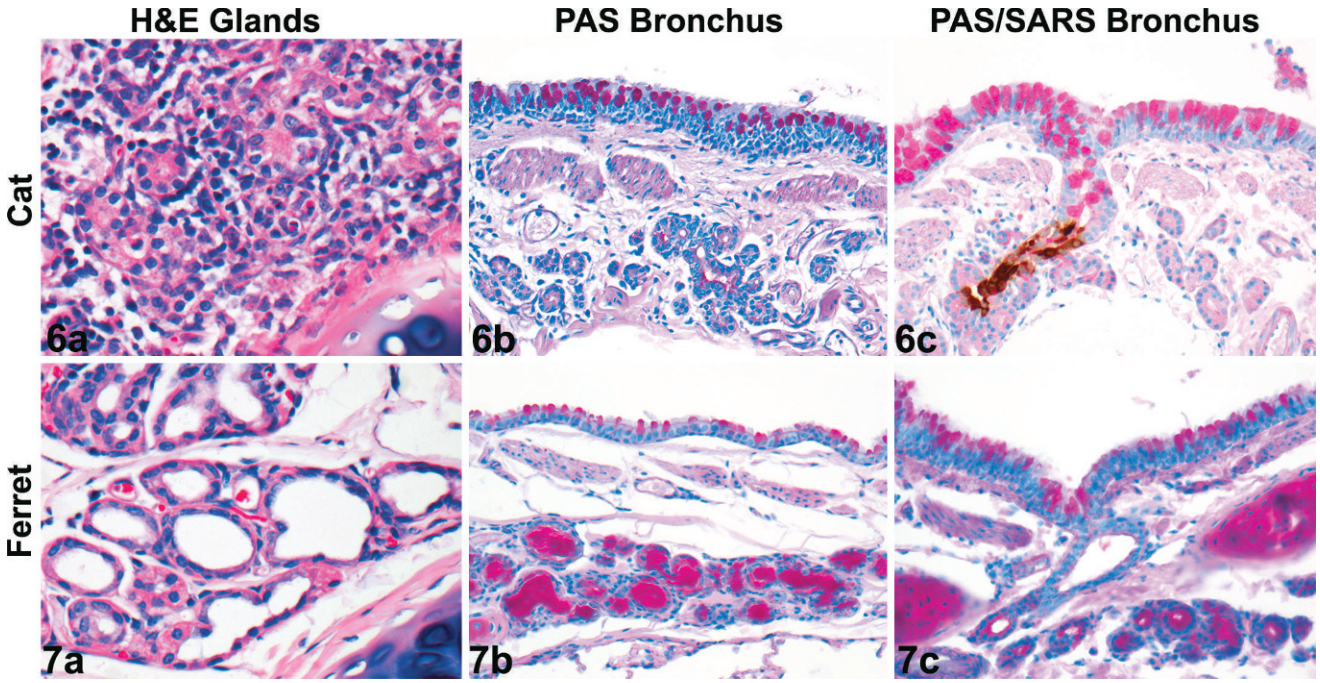

Figs. 6,7. Bronchus. Histologic, histochemical, and immunohistochemical staining of bronchi comparing cats and ferrets infected with SARS-CoV. **Fig. 6a.** Cat No. 1. Moderate lymphoplasmacytic bronchoadenitis with mild necrosis of glandular epithelial cells. HE. **Fig. 6b.** Cat No. 1. Few PAS-positive cells in bronchial submucosal glands and scant mucus in acinar lumina. **Fig. 6c.** Cat No. 3. SARS-CoV antigen expression in serous glandular epithelial cells. Double staining with PAS and immunoperoxidase. **Fig. 7a.** Ferret No. 2. No lesions in bronchial submucosal glands. HE. **Fig. 7b.** Ferret No. 3. Many PAS-positive cells in bronchial submucosal glands and abundant mucus in acinar lumina. PAS. **Fig. 7c.** Ferret No. 2. Lack of SARS-CoV antigen expression. Double staining with PAS and immunoperoxidase.

exclude macrophages (Figs. 13–15). The identity of SARS-CoV-antigen-positive serous cells in the tracheo-bronchial submucosal glands was based on the central-to-paracentral round nucleus and finely granular cytoplasm. It was confirmed by double staining with PAS: serous cells showed no or only weak staining with PAS, in contrast to intense staining of mucous cells also present in these glands (Figs. 6, 7). In the other tissues, a few enterocytes in the ileum had expression of SARS-CoV antigen, but only in the intestine of cat No. 2.

In all ferrets, SARS-CoV antigen expression was limited to the respiratory tract, where it was seen mainly in type II pneumocytes (Figs. 8–11), and rarely in type I pneumocytes and alveolar macrophages. Again, the identity of SARS-CoV-antigen-positive type I and type II pneumocytes was determined by their morphology and double staining with pankeratin (Figs. 13–15). Neither ferrets nor cats had viral antigen expression in the other tissues. Virus antigen expression was present in positive tissue controls and absent in negative tissue as well as isotype and omission controls.

The expression of SARS-CoV antigen in the respiratory tract of both cats and ferrets was usually associated with the presence of histologic lesions. The level of SARS-CoV antigen expression in the lungs of ferrets and cats showed no significant differences ($F = 1.34$, $P = .29$) (Fig. 12).

ACE2 expression

Expression of ACE2, visible as diffuse red staining of the cytoplasm and cell membrane, differed between the respiratory tract of cats and ferrets (Table 1, Figs. 1–4, 8–11). In cats, strong ACE2 expression was seen mainly in tracheal and bronchial goblet cells (Figs. 1, 2), serous epithelial cells of tracheo-bronchial submucosal glands (Figs. 1, 2), and type I and type II pneumocytes (Fig. 4); moderate expression was seen in tracheal, bronchial, and bronchiolar ciliated cells, bronchiolar nonciliated cells, and mucous cells of the tracheo-bronchial submucosal glands (Figs. 1–3); and weak expression was seen in alveolar macrophages. In addition, strong ACE2 expression was seen in the endothelium and smooth muscle of pulmonary blood vessels. In ferrets, the pattern of ACE2 expression resembled that in cats, except that it was absent in type I pneumocytes and in

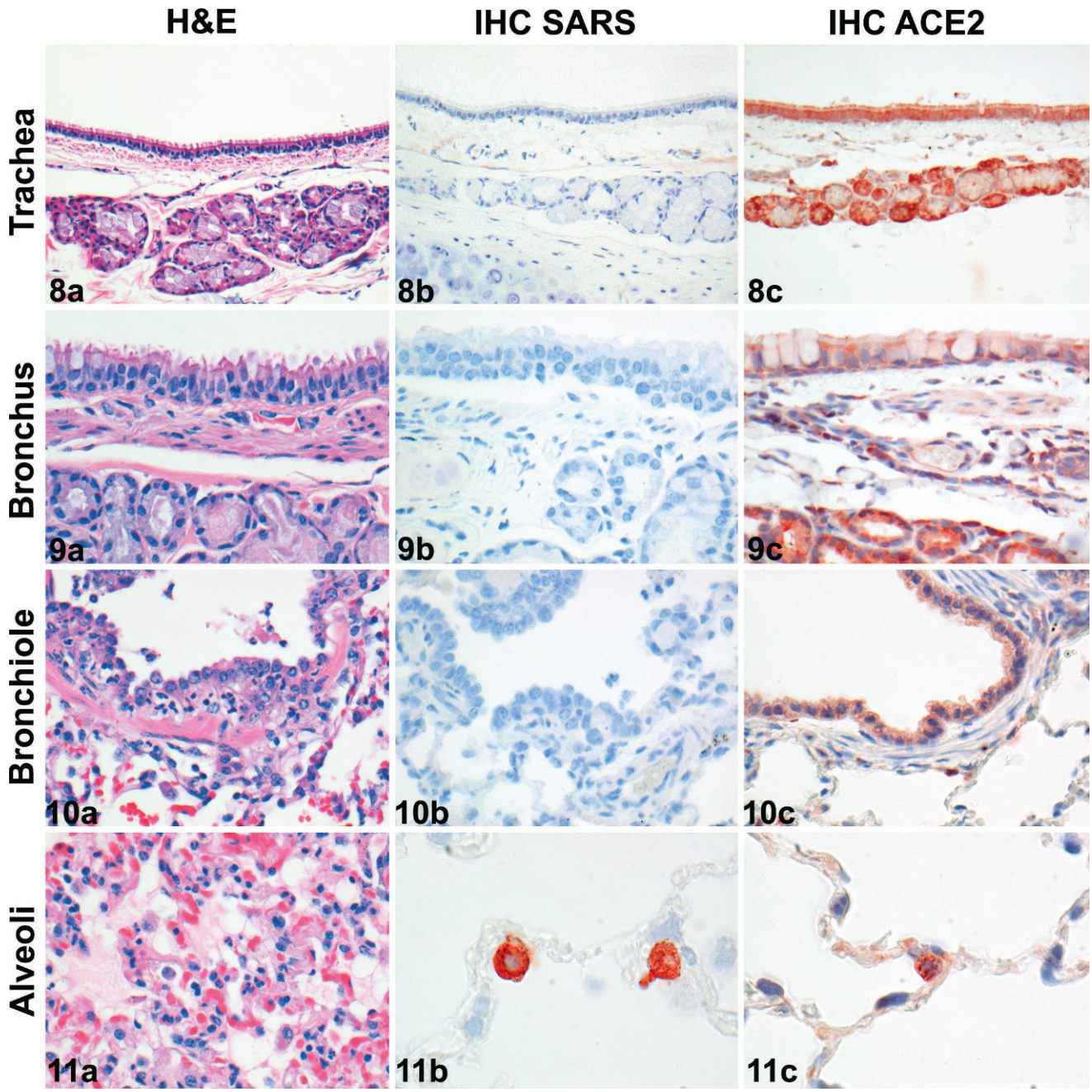

Figs. 8–11. Respiratory tract. Histologic and immunohistochemical staining for SARS-CoV antigen and ACE2 in SARS-CoV–infected ferrets and control ferrets. Detailed descriptions can be found in the text. **Fig. 8a.** Trachea; ferret No. 2. No lesions. HE. **Fig. 8b.** Trachea; ferret No. 2. Lack of SARS-CoV antigen expression. Immunoperoxidase with hematoxylin counterstain. **Fig. 8c.** Trachea; control ferret. ACE2 expression in epithelial cells of mucosa and submucosal glands. Immunoperoxidase with hematoxylin counterstain. **Fig. 9a.** Bronchus; ferret No. 3. No lesions. HE. **Fig. 9b.** Bronchus; ferret No. 3. Lack of SARS-CoV antigen expression. Immunoperoxidase with hematoxylin counterstain. **Fig. 9c.** Bronchus; control ferret. ACE2 expression in epithelial cells of mucosa and submucosal glands. Immunoperoxidase with hematoxylin counterstain. **Fig. 10a.** Bronchiole; ferret No. 2. Mild lymphoplasmacytic and neutrophilic bronchiolitis. HE. **Fig. 10b.** Bronchiole; ferret No. 2. Lack of SARS-CoV antigen expression. Immunoperoxidase with hematoxylin counterstain. **Fig. 10c.** Bronchiole; control ferret. ACE2 expression in epithelial cells of mucosa. Immunoperoxidase with hematoxylin counterstain. **Fig. 11a.** Alveoli; ferret No. 3. DAD with intraluminal protein. HE. **Fig. 11b.** Alveoli; ferret No. 3. SARS-CoV antigen expression in type II pneumocytes. Immunoperoxidase with hematoxylin counterstain. **Fig. 11c.** Alveoli; ferret. ACE2 expression in type II pneumocytes. Immunoperoxidase with hematoxylin counterstain.

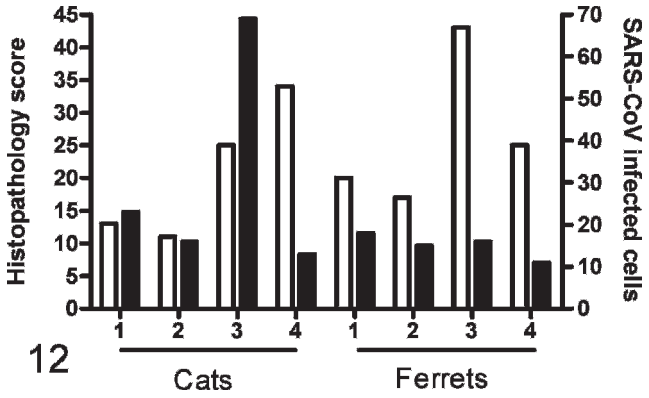

Fig. 12. Semiquantitative scoring of histologic lesions (white bars) and SARS-CoV antigen expression (black bars) in the lung. These scores did not differ significantly between cats and ferrets.

tracheal and bronchial goblet cells (Figs. 8–11). In human trachea, the ACE2 expression was stronger in serous cells than in mucous cells of mucosa and submucosal glands.

Discussion

The localization, character, and severity of respiratory tract lesions from acute SARS-CoV infection in cats and ferrets show both similarities to and differences from those in acute human cases.[4,7,11,27,33] First, the localization of the lesions in cats and ferrets is similar to that in humans: in all three species, the lesions affect mainly the alveoli and bronchioles. A clear difference is SARS-CoV–associated tracheo-bronchoadenitis, which we observed in cats, but which has not been reported in humans. Second, the character of the lesions in alveoli and bronchioles of cats and ferrets shows some similarities to that of humans. In all three species, these lesions are characterized by necrosis and subsequent hyperplasia of alveolar and bronchiolar epithelium, infiltration by neutrophils, and increased numbers of alveolar macrophages. In humans and ferrets, proteinaceous exudate was seen in alveolar and bronchiolar lumina. A notable difference is the lack of syncytia in the pulmonary lesions of cats and ferrets, whereas this feature is considered characteristic for the disease in humans. Third, the severity of the lesions in cats and ferrets shows the most marked difference from that in humans. The pulmonary lesions in cats and ferrets are multifocal, in contrast to the more diffuse lesions in humans. Also, cats and ferrets lack fibrin exudation and hyaline membrane formation, both of which are features of severe damage to the alveolar septum, while these features are commonly reported for human SARS. However, these differences in severity are largely a reflection of the fact that pathologic reports of human SARS are generally limited to fatal cases, which only comprise about 10% of the total number of confirmed cases.[29] It is likely that many people who recovered from SARS had less severe respiratory tract lesions. Overall, this comparison suggests that SARS-CoV infections in cats and ferrets are suitable animal models to study the pathogenesis and pathology of human SARS in general. However, in their present form they do not replicate the lesions of fatal cases of human SARS. Adapting this virus to cats and ferrets might increase its pathogenicity, as has been done for mice.[30]

Tracheo-bronchoadenitis caused by SARS-CoV infection is a novel finding, with potentially important implications for SARS pathogenesis and SARS-CoV excretion. Pathogenesis of SARS could be affected because the mucus produced by tracheo-bronchial submucosal glands is an important part of the mucociliary escalator that removes foreign material from the airways. Inflammation of these glands could reduce the efficiency of this

Table 1. Expression of ACE2 and SARS-CoV antigen in the respiratory tract of cats, ferrets, and humans with SARS.

		Tissues and Cell Types				
		Alveolus			Bronchiole	
Species	Antigens	Type I Pneumocyte	Type II Pneumocyte	Alveolar Macrophage	Ciliated Epithelial Cell	Nonciliated Epithelial Cell
Cat	ACE2	+++	+++	+	++	++
	SARS-CoV	+++	+++	+	+	−
Ferret	ACE2	−	+++	+	++	++
	SARS-CoV	−	+++	+	−	−
Human	ACE2[15]	++	+++	+	++	++
	SARS-CoV[3,29,33]	−	+++	+	−	−

NOTE: Abundance of ACE2 or SARS-CoV antigen expression: +++ = abundant; ++ = occasional; + = rare; − = absent.

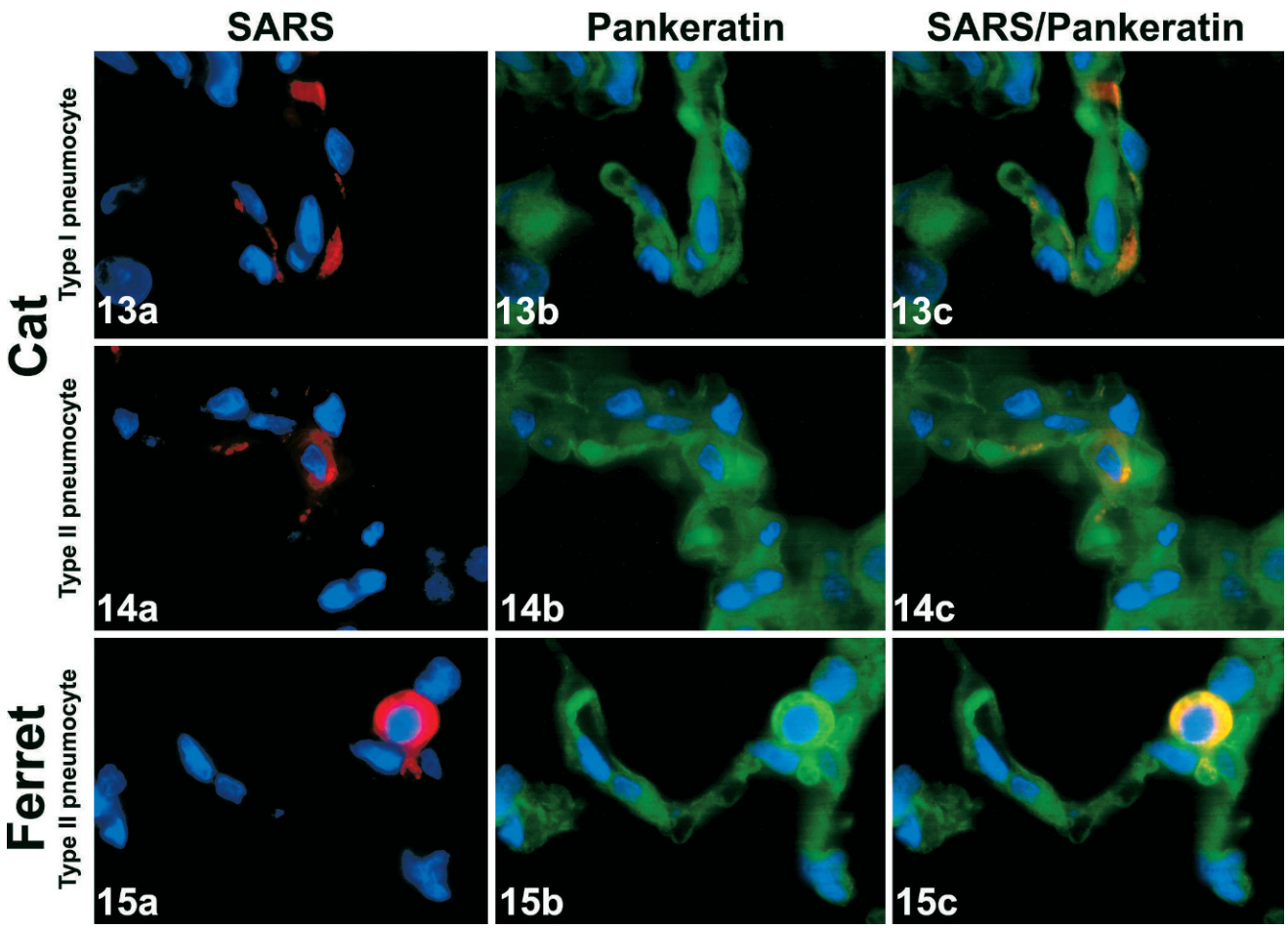

Figs. 13–15. Alveoli. Immunofluorescence double staining for SARS-CoV antigen and pankeratin in cats and ferrets infected with SARS-CoV antigen. **Fig. 13a.** Cat No. 3. Type I pneumocyte with SARS-CoV antigen expression (red). Immunofluorescence. **Fig. 13b.** Cat No. 3. Type I pneumocyte with pankeratin expression (green). Immunofluorescence. **Fig. 13c.** Cat No. 3. Type I pneumocyte with colocalization of SARS-CoV antigen and pankeratin (orange). Immunofluorescence. **Fig. 14a.** Cat No. 3. Type II pneumocyte with SARS-CoV antigen expression (red). Immunofluorescence. **Fig. 14b.** Cat No. 3. Type II pneumocyte with pankeratin expression (green). Immunofluorescence. **Fig. 14c.** Cat No. 3. Type II pneumocyte with colocalization of SARS-CoV antigen and pankeratin (orange). Immunofluorescence. **Fig. 15a.** Ferret No. 2. Type II pneumocyte with SARS-CoV antigen expression (red). Immunofluorescence. **Fig. 15b.** Cat No. 2. Type II pneumocyte with pankeratin expression (green). Immunofluorescence. **Fig. 15c.** Cat No. 2. Type II pneumocyte with colocalization of SARS-CoV antigen and pankeratin (orange). Immunofluorescence.

Table 1. Extended.

Tissues and Cell Types							
Bronchus			Trachea			Pulmonary Blood Vessel	
Ciliated Epithelial Cell	Goblet Cell	Glandular Epithelial Cell	Ciliated Epithelial Cell	Goblet Cell	Glandular Epithelial Cell	Endothelial cell	Smooth Muscle Cell
++	+++	+++	++	+++	+++	++	++
+	–	+++	+	–	+++	–	–
++	–	+++	++	–	+++	++	++
–	–	–	–	–	–	–	–
++	–	+++	++	–	+++	++	++
–	–	–	–	–	–	–	–

defense system, thereby increasing the risk of lower respiratory tract infection by SARS-CoV and concurrent pathogens. Excretion of SARS-CoV might increase as a result of SARS-CoV infection of the tracheo-bronchial submucosal glands: virus secreted by these glands into the trachea and bronchi is more likely to be expectorated than virus produced lower in the respiratory tract.

The susceptibility of tracheo-bronchial submucosal glands to SARS-CoV infection shows clear host species differences, which may be relevant for human infection. Although the glands of both cats and ferrets expressed ACE2, only cat glands became infected and inflamed (Figs. 1, 5, 6). One explanation may be that ferret glands lack a cofactor for SARS-CoV replication, as discussed above. Another explanation may be species differences in the histologic architecture of the tracheo-bronchial submucosal glands. The glands of ferrets had a higher proportion of mucous cells and more mucus in the acinar lumina than those of cats (Figs. 6, 7), and this may have inhibited the attachment of SARS-CoV to target cells. Therefore, we hypothesize that SARS-CoV infects mainly serous cells. To our knowledge, SARS-associated tracheo-bronchoadenitis has not been reported in humans. However, the expression of SARS-CoV antigen in the tracheal and bronchial submucosal glands of fatal human cases[3] suggests that inflammation of these glands may be an as-yet-unreported feature of human SARS that requires further attention.

This study shows the importance of ACE2 expression for SARS-CoV infection in vivo. This is based on our observation that SARS-CoV antigen expression occurred only in ACE2-positive cells (Table 1, Figs. 1–4, 8–11). SARS-CoV S1 protein is reported to bind efficiently to both ferret and feline ACE2.[13,41] The importance of ACE2 expression is well illustrated by differences that we observed between cats and ferrets at the level of the alveoli: whereas cat type I pneumocytes abundantly expressed both ACE2 and SARS-CoV antigen, the absence of ACE2 expression in ferret type I pneumocytes corresponded with the absence of expression of SARS-CoV antigen (Figs. 1–4, 8–11). However, it must be realized that colocalization of ACE2 and SARS-CoV antigen expression is consistent with, but not proof of, a functional relationship. Also, several ACE2-positive cell types did not express SARS-CoV antigen (Table 1). Possible reasons for this could be that other receptors besides ACE2 are required for SARS-CoV attachment to the host cell, as is also described in humans.[9,17,23,39] For example, recent in vitro studies have shown that the presence of cathepsin L is required for productive SARS-CoV infection.[16,34] Alternatively, SARS-CoV may infect other cell types at an earlier or later stage of infection.

Alveolar macrophages in both cats and ferrets demonstrated weak expression of ACE2 and sparse expression of SARS-CoV antigen. This presence of SARS-CoV antigen indicates either virus infection of alveolar macrophages or, as is suggested for humans,[38,39] phagocytosis of viral antigen produced in other cells.

In conclusion, our study shows that SARS-CoV infections in cats and ferrets are suitable models for studying the pathology and pathogenesis of human SARS. We also have identified tracheo-bronchoadenitis in cats as a novel SARS-CoV–induced lesion, which could potentially occur in human SARS and affect the pathogenesis and virus excretion of this disease. Finally, we have shown in vivo that ACE2 expression is important for SARS-CoV infection and subsequent development of lesions in the respiratory tract.

Acknowledgements

We are grateful for the help of F. van der Panne with microphotographs and G. van Amerongen and R. Dias D'Ullois with animal experiments. This work was supported by European grant SP22-CT-2004-511060 (DISSECT).

References

1 Czub M, Weingartl H, Czub S, He R, Cao J: Evaluation of modified vaccinia virus Ankara based recombinant SARS vaccine in ferrets. Vaccine **23:** 2273–2279, 2005

2 Darnell ME, Plant EP, Watanabe H, Byrum R, St Claire M, Ward JM, Taylor DR: Severe acute respiratory syndrome coronavirus infection in vaccinated ferrets. J Infect Dis **196:**1329–1338, 2007

3 Ding Y, He L, Zhang Q, Huang Z, Che X, Hou J, Wang H, Shen H, Qiu L, Li Z, Geng J, Cai J, Han H, Li X, Kang W, Weng D, Liang P, Jiang S: Organ distribution of severe acute respiratory syndrome (SARS) associated coronavirus (SARS-CoV) in SARS patients: implications for pathogenesis and virus transmission pathways. J Pathol **203:**622–630, 2004

4 Ding Y, Wang H, Shen H, Li Z, Geng J, Han H, Cai J, Li X, Kang W, Weng D, Lu Y, Wu D, He L, Yao K: The clinical pathology of severe acute respiratory syndrome (SARS): a report from China. J Pathol **200:**282–289, 2003

5 Drosten C, Gunther S, Preiser W, van der Werf S, Brodt HR, Becker S, Rabenau H, Panning M, Kolesnikova L, Fouchier RA, Berger A, Burguiere AM, Cinatl J, Eickmann M, Escriou N, Grywna K,

Kramme S, Manuguerra JC, Muller S, Rickerts V, Sturmer M, Vieth S, Klenk HD, Osterhaus AD, Schmitz H, Doerr HW: Identification of a novel coronavirus in patients with severe acute respiratory syndrome. N Engl J Med **348:**1967–1976, 2003

6 Fouchier RA, Kuiken T, Schutten M, Van Amerongen G, van Doornum GJ, van den Hoogen BG, Peiris M, Lim W, Stohr K, Osterhaus AD: Aetiology: Koch's postulates fulfilled for SARS virus. Nature **423:**240, 2003

7 Franks TJ, Chong PY, Chui P, Galvin JR, Lourens RM, Reid AH, Selbs E, McEvoy CP, Hayden CD, Fukuoka J, Taubenberger JK, Travis WD: Lung pathology of severe acute respiratory syndrome (SARS): a study of 8 autopsy cases from Singapore. Hum Pathol **34:**743–748, 2003

8 Glass WG, Subbarao K, Murphy B, Murphy PM: Mechanisms of host defense following severe acute respiratory syndrome–coronavirus (SARS-CoV) pulmonary infection of mice. J Immunol **173:**4030–4039, 2004

9 Gramberg T, Hofmann H, Moller P, Lalor PF, Marzi A, Geier M, Krumbiegel M, Winkler T, Kirchhoff F, Adams DH, Becker S, Munch J, Pohlmann S: LSECtin interacts with filovirus glycoproteins and the spike protein of SARS coronavirus. Virology **340:**224–236, 2005

10 Greenough TC, Carville A, Coderre J, Somasundaran M, Sullivan JL, Luzuriaga K, Mansfield K: Pneumonitis and multi-organ system disease in common marmosets (*Callithrix jacchus*) infected with the severe acute respiratory syndrome–associated coronavirus. Am J Pathol **167:**455–463, 2005

11 Gu J, Gong E, Zhang B, Zheng J, Gao Z, Zhong Y, Zou W, Zhan J, Wang S, Xie Z, Zhuang H, Wu B, Zhong H, Shao H, Fang W, Gao D, Pei F, Li X, He Z, Xu D, Shi X, Anderson VM, Leong AS: Multiple organ infection and the pathogenesis of SARS. J Exp Med **202:**415–424, 2005

12 Gu J, Korteweg C: Pathology and pathogenesis of severe acute respiratory syndrome. Am J Pathol **170:**1136–1147, 2007

13 Guo H, Guo A, Wang C, Yan B, Lu H, Chen H: Expression of feline angiotensin converting enzyme 2 and its interaction with SARS-CoV S1 protein. Res Vet Sci (in press)

14 Haagmans BL, Kuiken T, Martina BE, Fouchier RA, Rimmelzwaan GF, Van Amerongen G, van Riel D, de Jong T, Itamura S, Chan KH, Tashiro M, Osterhaus AD: Pegylated interferon-alpha protects type 1 pneumocytes against SARS coronavirus infection in macaques. Nat Med **10:**290–293, 2004

15 Hamming I, Timens W, Bulthuis ML, Lely AT, Navis GJ, van Goor H: Tissue distribution of ACE2 protein, the functional receptor for SARS coronavirus. A first step in understanding SARS pathogenesis. J Pathol **203:**631–637, 2004

16 Huang IC, Bosch BJ, Li F, Li W, Lee KH, Ghiran S, Vasilieva N, Dermody TS, Harrison SC, Dormitzer PR, Farzan M, Rottier PJ, Choe H: SARS coronavirus, but not human coronavirus NL63, utilizes cathepsin L to infect ACE2-expressing cells. J Biol Chem **281:**3198–3203, 2006

17 Jeffers SA, Tusell SM, Gillim-Ross L, Hemmila EM, Achenbach JE, Babcock GJ, Thomas WD Jr, Thackray LB, Young MD, Mason RJ, Ambrosino DM, Wentworth DE, Demartini JC, Holmes KV: CD209L (L-SIGN) is a receptor for severe acute respiratory syndrome coronavirus. Proc Natl Acad Sci U S A **101:**15748–15753, 2004

18 Kuba K, Imai Y, Rao S, Gao H, Guo F, Guan B, Huan Y, Yang P, Zhang Y, Deng W, Bao L, Zhang B, Liu G, Wang Z, Chappell M, Liu Y, Zheng D, Leibbrandt A, Wada T, Slutsky AS, Liu D, Qin C, Jiang C, Penninger JM: A crucial role of angiotensin converting enzyme 2 (ACE2) in SARS coronavirus-induced lung injury. Nat Med **11:**875–879, 2005

19 Kuiken T, Fouchier RA, Schutten M, Rimmelzwaan GF, Van Amerongen G, van Riel D, Laman JD, de Jong T, van Doornum G, Lim W, Ling AE, Chan PK, Tam JS, Zambon MC, Gopal R, Drosten C, van der Werf S, Escriou N, Manuguerra JC, Stohr K, Peiris JS, Osterhaus AD: Newly discovered coronavirus as the primary cause of severe acute respiratory syndrome. Lancet **362:**263–270, 2003

20 Li W, Moore MJ, Vasilieva N, Sui J, Wong SK, Berne MA, Somasundaran M, Sullivan JL, Luzuriaga K, Greenough TC, Choe H, Farzan M: Angiotensin-converting enzyme 2 is a functional receptor for the SARS coronavirus. Nature **426:**450–454, 2003

21 Li W, Shi Z, Yu M, Ren W, Smith C, Epstein JH, Wang H, Crameri G, Hu Z, Zhang H, Zhang J, McEachern J, Field H, Daszak P, Eaton BT, Zhang S, Wang LF: Bats are natural reservoirs of SARS-like coronaviruses. Science **310:**676–679, 2005

22 Martina BE, Haagmans BL, Kuiken T, Fouchier RA, Rimmelzwaan GF, Van Amerongen G, Peiris JS, Lim W, Osterhaus AD: Virology: SARS virus infection of cats and ferrets. Nature **425:**915, 2003

23 Marzi A, Gramberg T, Simmons G, Moller P, Rennekamp AJ, Krumbiegel M, Geier M, Eisemann J, Turza N, Saunier B, Steinkasserer A, Becker S, Bates P, Hofmann H, Pohlmann S: DC-SIGN and DC-SIGNR interact with the glycoprotein of Marburg virus and the S protein of severe acute respiratory syndrome coronavirus. J Virol **78:**12090–12095, 2004

24 Nagata N, Iwata N, Hasegawa H, Fukushi S, Yokoyama M, Harashima A, Sato Y, Saijo M, Morikawa S, Sata T: Participation of both host and virus factors in induction of severe acute respiratory syndrome (SARS) in F344 rats infected with SARS coronavirus. J Virol **81:**1848–1857, 2007

25 Nicholls JM, Poon LL, Lee KC, Ng WF, Lai ST, Leung CY, Chu CM, Hui PK, Mak KL, Lim W, Yan KW, Chan KH, Tsang NC, Guan Y, Yuen KY, Peiris JS: Lung pathology of fatal severe acute respiratory syndrome. Lancet **361:**1773–1778, 2003

26 Nikitin AY, Alcaraz A, Anver MR, Bronson RT, Cardiff RD, Dixon D, Fraire AE, Gabrielson EW, Gunning WT, Haines DC, Kaufman MH, Linnoila RI, Maronpot RR, Rabson AS, Reddick RL, Rehm S, Rozengurt N, Schuller HM, Shmidt EN, Travis WD, Ward JM, Jacks T: Classification of proliferative pulmonary lesions of the mouse: recommendations of the mouse models of human cancers consortium. Cancer Res **64:**2307–2316, 2004
27 Pei F, Zheng J, Gao ZF, Zhong YF, Fang WG, Gong EC, Zou WZ, Wang SL, Gao DX, Xie ZG, Lu M, Shi XY, Liu CR, Yang JP, Wang YP, Han ZH, Shi XH, Dao WB, Gu J: Lung pathology and pathogenesis of severe acute respiratory syndrome: a report of six full autopsies. Zhonghua Bing Li Xue Za Zhi **34:**656–660, 2005
28 Peiris JS, Lai ST, Poon LL, Guan Y, Yam LY, Lim W, Nicholls J, Yee WK, Yan WW, Cheung MT, Cheng VC, Chan KH, Tsang DN, Yung RW, Ng TK, Yuen KY: Coronavirus as a possible cause of severe acute respiratory syndrome. Lancet **361:**1319–1325, 2003
29 Peiris JS, Yuen KY, Osterhaus AD, Stohr K: The severe acute respiratory syndrome. N Engl J Med **349:**2431–2441, 2003
30 Roberts A, Deming D, Paddock CD, Cheng A, Yount B, Vogel L, Herman BD, Sheahan T, Heise M, Genrich GL, Zaki SR, Baric R, Subbarao K: A mouse-adapted SARS-coronavirus causes disease and mortality in BALB/c mice. PLoS Pathog **3:**e5, 2007
31 Roberts A, Paddock C, Vogel L, Butler E, Zaki S, Subbarao K: Aged BALB/c mice as a model for increased severity of severe acute respiratory syndrome in elderly humans. J Virol **79:**5833–5838, 2005
32 Roberts A, Vogel L, Guarner J, Hayes N, Murphy B, Zaki S, Subbarao K: Severe acute respiratory syndrome coronavirus infection of golden Syrian hamsters. J Virol **79:**503–511, 2005
33 Shieh WJ, Hsiao CH, Paddock CD, Guarner J, Goldsmith CS, Tatti K, Packard M, Mueller L, Wu MZ, Rollin P, Su IJ, Zaki SR: Immunohistochemical, in situ hybridization, and ultrastructural localization of SARS-associated coronavirus in lung of a fatal case of severe acute respiratory syndrome in Taiwan. Hum Pathol **36:**303–309, 2005
34 Simmons G, Gosalia DN, Rennekamp AJ, Reeves JD, Diamond SL, Bates P: Inhibitors of cathepsin L prevent severe acute respiratory syndrome coronavirus entry. Proc Natl Acad Sci U S A **102:**11876–11881, 2005
35 Subbarao K, Roberts A: Is there an ideal animal model for SARS? Trends Microbiol **14:**299–303, 2006
36 ter Meulen J, Bakker AB, van den Brink EN, Weverling GJ, Martina BE, Haagmans BL, Kuiken T, de Kruif J, Preiser W, Spaan W, Gelderblom HR, Goudsmit J, Osterhaus AD: Human monoclonal antibody as prophylaxis for SARS coronavirus infection in ferrets. Lancet **363:**2139–2141, 2004
37 To KF, Lo AW: Exploring the pathogenesis of severe acute respiratory syndrome (SARS): the tissue distribution of the coronavirus (SARS-CoV) and its putative receptor, angiotensin-converting enzyme 2 (ACE2). J Pathol **203:**740–743, 2004
38 To KF, Tong JH, Chan PK, Au FW, Chim SS, Chan KC, Cheung JL, Liu EY, Tse GM, Lo AW, Lo YM, Ng HK: Tissue and cellular tropism of the coronavirus associated with severe acute respiratory syndrome: an in-situ hybridization study of fatal cases. J Pathol **202:**157–163, 2004
39 Yang ZY, Huang Y, Ganesh L, Leung K, Kong WP, Schwartz O, Subbarao K, Nabel GJ: pH-dependent entry of severe acute respiratory syndrome coronavirus is mediated by the spike glycoprotein and enhanced by dendritic cell transfer through DC-SIGN. J Virol **78:**5642–5650, 2004
40 Ye J, Zhang B, Xu J, Chang Q, McNutt MA, Korteweg C, Gong E, Gu J: Molecular pathology in the lungs of severe acute respiratory syndrome patients. Am J Pathol **170:**538–545, 2007
41 Zamoto A, Taguchi F, Fukushi S, Morikawa S, Yamada YK: Identification of ferret ACE2 and its receptor function for SARS-coronavirus. Adv Exp Med Biol **581:**519–522, 2006

Request reprints from Dr. Thijs Kuiken, Department of Virology, Erasmus Medical Center, Dr. Molewaterplein 50, 3015 GE Rotterdam (The Netherlands). E-mail: t.kuiken@erasmusmc.nl.